

## Parascholzite, a new mineral from Hagendorf, Bavaria, and its relationship to scholzite

B. DARKO STURMAN

Department of Mineralogy and Geology  
Royal Ontario Museum, Toronto, Ontario M5S 2C6, Canada

ROLAND C. ROUSE

Department of Geological Sciences  
University of Michigan, Ann Arbor, Michigan 48109

AND PETE J. DUNN

Department of Mineral Sciences  
Smithsonian Institution, Washington, D.C. 20560

### Abstract

The new mineral parascholzite,  $\text{CaZn}_2(\text{PO}_4)_2 \cdot 2\text{H}_2\text{O}$ , from Hagendorf, Bavaria, is monoclinic,  $Cc$  or  $C2/c$ , with  $a = 17.864(5)$ ,  $b = 7.422(2)$ ,  $c = 6.674(2)\text{\AA}$ , and  $\beta = 106^\circ 27'(1)'$ . Comparison with scholzite from Reaphook Hill, South Australia shows that the two minerals are dimorphous, scholzite being orthorhombic,  $Pbc2_1$ , with  $a = 17.178(8)$ ,  $b = 22.24(1)$ , and  $c = 6.681(3)\text{\AA}$ . Aside from its monoclinic distortion, the unit cell of parascholzite corresponds to the subcell of scholzite, which has  $B = b/3 = 7.413\text{\AA}$  and symmetry  $Pbcn$ . Both scholzite and parascholzite are derived from this basic structure. Weak diffuse nonrational superstructure reflections from parascholzite indicate a supercell with  $c' \approx 3c$ . Parascholzite is invariably twinned with  $\{100\}$  as both the twin and composition plane.

Parascholzite is white to colorless with a white streak. The specific gravity is 3.12 (obs.) and density  $3.10\text{ g/cm}^3$  (calc.). Hardness (Mohs) is 4. Optically it is biaxial (+) with  $2V_z = 25^\circ$  (obs.),  $r > v$ ,  $\alpha = 1.587$ ,  $\beta = 1.588$ ,  $\gamma = 1.603$ ; the orientation of the indicatrix is  $b||X$  and  $c \wedge Z = 13^\circ$  in the acute angle between  $c$  and  $a$ .

Physical, optical, and morphological properties of the two minerals are similar, but parascholzite may be distinguished by its inclined extinction and unique powder diffraction lines at  $4.158$  and  $2.779\text{\AA}$ . Scholzite and parascholzite commonly form syntaxial intergrowths with  $\{100\}$  the composition plane. Much previously published scholzite data were obtained from these intergrowths or from parascholzite itself, which explains some of the confusion in the literature on the former mineral. A new set of physical, optical and crystallographic data for Australian scholzite is presented. Worldwide occurrences of the two minerals are also reviewed.

### Introduction

During our study of the new mineral parascholzite, the monoclinic dimorph of scholzite ( $\text{CaZn}_2(\text{PO}_4)_2 \cdot 2\text{H}_2\text{O}$ ), it became evident that some of the published data for the latter mineral had been obtained from mixtures of the two. In this report we shall first describe the new mineral parascholzite, then give a new set of data for scholzite, and finally describe the syntaxial intergrowths of scholzite and

parascholzite, whose previously unsuspected existence has produced some confusion in the literature.

### Parascholzite

#### Introduction

Parascholzite was discovered on pegmatite specimens from Hagendorf, Bavaria, West Germany, where it occurs as well-developed crystals less than  $1.0\text{ mm}$  in size associated with vivianite, phospho-

phyllite and strengite. It was pointed out to one of the authors (PJD) several years ago by Mrs. Kay Robertson, who noted that it was then mislabelled as fluellite and suggested that it was probably scholzite. Further investigation indicated that the new species was indeed very closely related to scholzite but was crystallographically different.

Parascholzite was first identified on a specimen in the Smithsonian collection, NMNH B14345. Another specimen, NMNH B14318, had better developed crystals and these were therefore used for the characterization of the mineral. We have no information as to whether these specimens were collected at Hagendorf Nord or Hagendorf Süd. However, a specimen in the Royal Ontario Museum collection, M 34603, from Hagendorf Süd was found to contain the new mineral. Subsequently, parascholzite was discovered in Smithsonian specimen (NMNH 106411) from Hagendorf Nord, but in this case it occurred as microscopic lamellae in crystals from the type specimen of scholzite. Examination of published powder patterns of scholzite from other localities indicates that parascholzite also occurs, in some form, at all known scholzite locations.

The name is for the dimorphic relationship to scholzite. The new mineral and the name have been approved by the Commission on New Minerals and Mineral Names, I.M.A. Type material is deposited in the Smithsonian Institution, Washington, D.C. 20560 under the catalog numbers B14345 and B14318.

### Crystallography

Parascholzite occurs as tabular prismatic crystals twinned by reflection on  $\{100\}$ , which is also the composition plane. The crystals are flattened on  $\{100\}$  and elongated parallel to  $[001]$ . Most crystals studied were composed of thin polysynthetically twinned lamellae, but a few simple twins consisted of only two individuals. A crystal of the latter type (Fig. 1) was chosen for study with the polarizing microscope, optical goniometer, and precession camera. After determining the twin relations, the crystal was attached to a glass slide and the smaller individual of the twin was ground away using the techniques for thin section preparation. The remaining untwinned crystal was then re-examined with the microscope and precession camera.

The forms observed on five crystals with the optical goniometer are given in Table 1. The faces of polysynthetically twinned crystals can be assigned two different sets of Miller indices. In the angle table (Table 1) measured values of  $\phi$  and  $\rho$  are compared

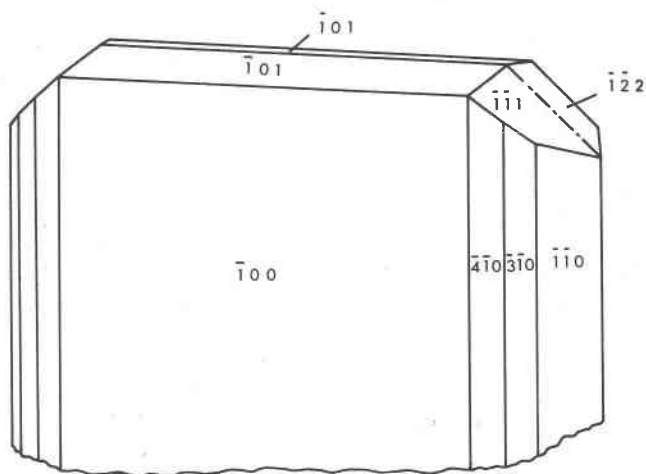


Fig. 1. A simple twin of parascholzite from Hagendorf. The front individual is three times larger than the rear individual. The face  $g$  ( $\bar{1}\bar{1}\bar{1}$ ) of the front individual continues in the rear crystal as the face  $f$  ( $\bar{1}\bar{2}\bar{2}$ ) (see text).

to the calculated values for the two sets of lamellae, one having the positive end of the  $a$ -axis pointing towards the observer (orientation I) and the other with the negative end pointing towards the observer (orientation II). The stereographic projections of the forms for the two sets of lamellae appear in Fig. 2.

The habit of the polysynthetically twinned crystals (Fig. 3) also differs slightly from that of the simple twins (Fig. 1). The forms in Fig. 3 are for orientation I; the corresponding indices for the other set can be found in Table 1. Signals from some faces were of poor quality on all crystals examined, faces of the forms  $\{001\}$  and  $\{\bar{1}01\}$  (orientation I) being especially affected. Faces of forms  $\{310\}$  and  $\{410\}$  are narrow but give distinct signals. It appears that they are developed only on the simple twins.

The unit cell and space group of parascholzite were determined by the precession, Weissenberg and rotating crystal methods. The new mineral is monoclinic,  $Cc$  or  $C2/c$ , with  $a = 17.864(5)$ ,  $b = 7.422(2)$ ,  $c = 6.674(2)\text{\AA}$ ,  $\beta = 106^\circ 27'(1)$ , and  $V = 848.7\text{\AA}^3$ . There are four formula weights per cell. These unit cell parameters were refined from the Guinier powder diffraction data using silicon and quartz as internal standards. The intensities observed on the single-crystal photographs were used to index each powder reflection unambiguously. The powder diffraction patterns of scholzite and parascholzite are generally quite similar (Table 2), but enough differences exist to permit the unequivocal identification of each phase. The major diagnostic differences are the me-

Table 1. Angle table for a twinned crystal of parascholzite

Monoclinic, $a=17.864$ , $b=7.422$ , $c=6.674$ , $\beta=106^{\circ}27'$								
Twin plane and composition plane (100).								
Measured		Calculated						
$\phi$	$\rho$	Orientation I			Orientation II			$\rho$
		Form	$\phi$	$\rho$	Form	$\phi$	$\rho$	
$90^{\circ}$	$90^{\circ}$	a(100)	$90^{\circ}00'$	$90^{\circ}00'$	a(100)	$90^{\circ}00'$	$90^{\circ}00'$	
$23^{\circ}43'$	$90^{\circ}$	k(110)	$23^{\circ}25'$	$90^{\circ}00'$	k(110)	$23^{\circ}25'$	$90^{\circ}00'$	
$54^{\circ}$	$90^{\circ}$	m(310)	$52^{\circ}25'$	$90^{\circ}00'$	m(310)	$52^{\circ}25'$	$90^{\circ}00'$	
$59^{\circ}$	$90^{\circ}$	j(410)	$60^{\circ}00'$	$90^{\circ}00'$	j(410)	$60^{\circ}00'$	$90^{\circ}00'$	
$90^{\circ}$	$17^{\circ}$	c(001)	$90^{\circ}00'$	$16^{\circ}27'$	d( $\bar{3}02$ )	$-90^{\circ}00'$	$16^{\circ}07'$	
$90^{\circ}$	$8^{\circ}$	y( $\bar{1}01$ )	$-90^{\circ}00'$	$5^{\circ}23'$	x( $\bar{1}02$ )	$90^{\circ}00'$	$5^{\circ}44'$	
$5^{\circ}25'$	$41^{\circ}55'$	g( $\bar{1}11$ )	$-5^{\circ}59'$	$42^{\circ}07'$	f( $\bar{1}22$ )	$6^{\circ}22'$	$42^{\circ}08'$	

Note: Orientation I is for the lamellae with the positive end of the a-axis pointed towards the observer; the lamellae of the orientation II are rotated by  $180^{\circ}$  around the c-axis.

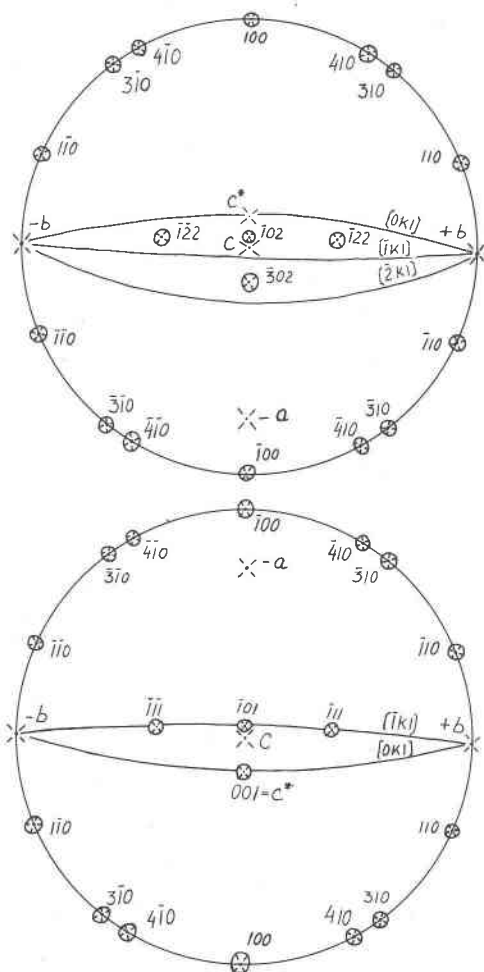


Fig. 2. Stereographic projections of the forms and crystallographic axes for the two sets of lamellae of polysynthetically twinned parascholzite crystals.

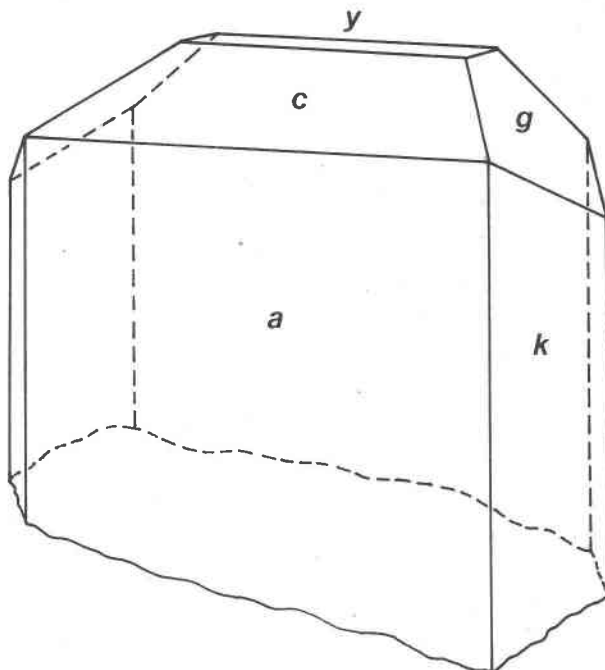


Fig. 3. A polysynthetically twinned parascholzite crystal from Hagendorf.

dium intensity lines at 4.158 and 2.779 Å in parascholzite and the unique scholzite line at 2.689 Å.

Aside from its monoclinic distortion, the unit cell of parascholzite corresponds dimensionally to the subcell of scholzite for which  $A = a = 17.178(8)$ ,  $B = b/3 = 7.413(4)$ , and  $C = c = 6.681(3)$  Å, these parameters being determined from Australian scholzite. The subcell symmetry is  $Pbcn$ , which is reduced to  $Pbc2_1$  in the supercell by small displacements of the atoms from their ideal substructure positions (Taxer, 1975). In parascholzite there is a  $c$ -glide in the (010) plane. Moreover, reflections  $0kl$  with  $k$  odd are unobserved, implying the existence of a pseudo  $b$ -glide in the (100) plane. Parascholzite thus contains all of the glide planes of  $Pbcn$  (at least approximately) and this, taken with the marked similarity in cell parameters, strongly implies that parascholzite as well as scholzite is a derivative of the basic  $Pbcn$  structure.

A crystallographic feature of parascholzite not found in any scholzite crystal examined by us nor mentioned by previous workers (Strunz and Tennyson, 1956; Taxer, 1970; Czaya, 1972; Hill *et al.*, 1973; Taxer, 1975) is a set of weak diffuse superstructure reflections, which seem to require the tripling of the  $c$  parameter. However, careful measurements of the positions of these reflections on an  $h0l$  precession photograph taken with  $CuK\alpha$  radiation proves that

Table 2. X-ray powder diffraction data for parascholzite from Hagendorf and scholzite from Reaphook Hill

Parascholzite				Scholzite				Parascholzite				Scholzite			
a 17.864, b 7.422, c 6.674				a 17.178, b 22.24, c 6.681				I	d <sub>obs</sub>	d <sub>cal</sub>	hkl	I	d <sub>obs</sub>	d <sub>cal</sub>	hkl
$\beta$ 106°27'								1	2.180	2.180	$\bar{7}12$	5	2.147	2.147	800
C2/c or Cc				Pbc2 <sub>1</sub>				1	2.082	2.081	$\bar{6}22$	5	2.086	2.086	632
I	d <sub>obs</sub>	d <sub>cal</sub>	hkl	I	d <sub>obs</sub>	d <sub>cal</sub>	hkl	5	2.005	2.006	530	10	2.006	2.006	590
100	8.55	8.57	200	100	8.55	8.59	200	5	1.989	1.990	$\bar{5}12$	5	1.972	1.971	831
10	6.80	6.81	$\bar{1}10$	10	6.81	6.81	130	20	1.908	1.911	821	40	1.909	1.911	732
5	4.95	4.95	111	30	4.53	4.53	330			1.908	132			1.909	063
30	4.53	4.53	310	60	4.300	4.297	231	1	1.829	1.829	$\bar{9}12$	20	1.814	1.813	240
5	4.424	4.422	111			4.295	400			1.907	223				
10	4.287	4.283	400	5	3.748	3.750	331				$\bar{7}12$				
50	4.158	4.162	$\bar{3}11$	10	3.709	3.707	060	5	1.675	1.678	712				
10	3.709	3.711	020	40	3.404	3.403	260	20	1.660	1.661	$\bar{4}04$				
40	3.406	3.405	220	5	3.339	3.340	002			1.660	204				
10	3.360	3.357	311	1	3.277	3.279	102				$\bar{2}42$				
1	3.313	3.322	202	10	3.243	3.247	431	5	1.619	1.620	242				
5	3.207	3.210	021	30	3.182	3.185	161	5	1.603	1.605	042				
		3.200	002	10	3.112	3.117	530			1.603	604				
20	3.153	3.157	$\bar{2}21$	10	3.112	3.113	202	5	1.601	1.601	441				
10	3.109	3.111	510	1	3.032	3.033	261			1.600	004				
10	3.005	3.004	$\bar{4}02$	5	2.880	2.885	302	10	1.584	1.586	532				
5	2.945	2.943	$\bar{3}12$	10	2.870	2.870	232	1	1.577	1.579	442				
				70	2.805	2.806	460			1.577	133				
								5	1.554	1.556	$10\cdot2\cdot0$				
										1.553	$11\cdot1\cdot2$				
80	2.804	2.805	420	30	2.689	2.689	332	1	1.524						
40	2.779	2.779	$\bar{1}12$	5	2.640	2.637	402	5	1.515						
5	2.766	2.764	421	5	2.592	2.587	461	1	1.508						
10	2.752	2.753	202					5	1.500						
				20	2.481	2.484	432	10	1.470						
								1	1.435						
30	2.586	2.588	512					5	1.413						
1	2.553	2.552	511					5	1.390						
1	2.511	2.513	$\bar{5}02$												
10	2.475	2.475	$\bar{2}22$	5	2.456	2.456	162								
				10	2.385	2.384	262								
5	2.424	2.424	022	10	2.331	2.330	730								
1	2.374	2.374	312	1	2.301	2.297	191								
5	2.332	2.335	422	1	2.271	2.277	362								
5	2.325	2.324	710			2.269	390								
1	2.299	2.302	$\bar{6}21$	30	2.265	2.265	660								
20	2.263	2.263	620					1	1.276						
5	2.212	2.211	222					1	1.237						

Guinier camera, Cu K $\alpha$  radiation, intensities estimated visually, Si internal standard

they are not exactly  $\frac{1}{3}$  and  $\frac{2}{3}$  of the distance between adjacent reciprocal lattice rows of the  $c = 6.674\text{\AA}$  cell. There is a deviation of about 18 percent from their ideal positions, making the supercell parameter  $c'$  only approximately equal to  $3c$ . At present the structural significance of these reflections can only be surmised, but a study with high resolution transmission electron microscopy is planned in the hope of resolving this problem.

Taxer (1970) and (independently) Hill *et al.* (1973) noted extensive streaking of reflections parallel to  $a^*$

in scholzite. Since scholzite is a layer structure containing sheets of edge-sharing  $\text{PO}_4 + \text{ZnO}_4$  tetrahedra, the streaking was ascribed to stacking disorder of the sheets along [100]. Weissenberg photographs of parascholzite show this same streaking along  $a^*$ , lending further credence to the close structural relationship proposed for these two minerals.

#### Physical and optical properties

Parascholzite is white to colorless with a white streak and vitreous luster. The specific gravity of 3.12

$\pm 0.03$ , measured with heavy liquid techniques, compares well with the calculated density of  $3.10 \text{ g/cm}^3$  obtained from the ideal composition and the refined cell parameters. The Mohs hardness is approximately 4. There is no observable cleavage, but polysynthetically twinned crystals show a parting along the composition plane  $\{100\}$ . Parascholzite does not fluoresce in ultraviolet light.

Optical properties of parascholzite are summarized in Table 3 and Figure 4. The optic axial angle was determined with the universal stage. Refractive indices and the orientation of the indicatrix were determined on the spindle stage using sodium light and a crystal previously oriented by single-crystal X-ray diffraction methods. The principal vibration direction  $Z$  forms an angle of  $13^\circ$  with the  $c$ -axis and is in the acute angle between the  $a$ -axis and  $c$ -axis.

Using the Gladstone–Dale relationship, the constants of Mandarino (1976), and the chemical composition in Table 4, the specific refractivity was calculated to be  $K_c = 0.187$ . This compares well with the value  $K_p = 0.190$  calculated from the measured density and refractive indices.

#### Chemical composition

Parascholzite was chemically analyzed using an ARL-SEM-Q electron microprobe utilizing an operating voltage of 15 kV and a beam current of  $0.15 \mu\text{A}$ . The

data were corrected using Bence–Albee factors and a computer program. The standards used in the analysis were fluorapatite for Ca and P, synthetic ZnO for Zn, manganite for Mn, and hornblende for Fe. A microprobe scan indicated the absence of any elements with atomic number greater than nine, except for the ones reported here. Water was determined by the Penfield method. The resulting analysis is presented in Table 4. Using the refined cell parameters and measured density, the calculated formula of parascholzite is  $(\text{Ca}_{3.67}\text{Mn}_{0.32})_{\Sigma 3.99}(\text{Zn}_{7.92}\text{Fe}_{0.11})_{\Sigma 8.03}(\text{PO}_4)_{8.07} \cdot 7.88\text{H}_2\text{O}$ , in excellent agreement with the ideal formula  $\text{CaZn}_2(\text{PO}_4)_2 \cdot 2\text{H}_2\text{O}$  with  $Z = 4$ .

DTA and TGA curves of parascholzite were obtained with a Mettler Thermoanalyser. A 5 mg sample was heated at  $10^\circ/\text{min}$ . in a nitrogen atmosphere to  $600^\circ\text{C}$ . Three weight losses totaling 9.6 wt.%, are related to endothermic peaks at  $153^\circ$ ,  $313^\circ$ , and  $385^\circ\text{C}$ . An analysis of scholzite from Reaphook Hill gave practically identical curves.

### Scholzite

#### Introduction

Scholzite was first described from Hagendorf, Bavaria by Strunz (1950). The original description is of a monoclinic, pseudo-orthorhombic mineral with parameters  $a = 6.46$ ,  $b = 9.05$ ,  $c = 7.55$ ,  $\beta = 90^\circ$  and the

Table 3. Optical and crystallographic data for scholzite and parascholzite

	Scholzite Reaphook Hill		This study	Scholzite Hagendorf			Parascholzite Hagendorf
	This study	Hill 1973		Taxer 1974	Strunz 1956	Strunz 1950	
system	ortho	monoc	ortho	ortho	ortho	monoc	monoc
space group	Pbcm or Pbc2 <sub>1</sub>	P2 <sub>1</sub> /b	Pbcm or Pbc2 <sub>1</sub>	Pbc2 <sub>1</sub>	Pbmm or Pbnn		C2/c or Cc
a	17.178(8)	17.164(6)	17.161(7)	17.149(3)	17.14	6.46	17.864(5)
b	22.24(1)	22.244(8)	22.28(2)	22.236(2)	22.19	9.05	7.422(2)
c	6.681(3)	6.673(2)	6.691(6)	6.667(1)	6.61	7.55	6.674(2)
$\beta$		$90^\circ 00'$				$90^\circ$	$106^\circ 27(1)'$
$\delta$	1.597(2)		1.599(2)		1.596	1.604	1.603(2)
$\beta$	1.586(2)		1.587(2)		1.586	1.589	1.588(2)
$\alpha$	1.585(2)		1.585(2)		1.581	1.583	1.587(2)
optic sign	+		+		+	+	+
$2V_{\text{cal}}$	$2V_z = 34^\circ$		$2V_z = 45^\circ$		$2V_z = 71^\circ$	$2V_z = 65^\circ$	$2V_z = 29^\circ$
$2V_{\text{meas}}$	$2V_z = 33(2)^\circ$		$2V_z = 44(2)^\circ$		$2V_z = 70^\circ$	$2V_{z \text{ small}}$	$2V_z = 25(2)^\circ$
dispersion	$r > v$		$r > v$		$r > v$		$r > v$
orientation of the indicatrix	Z    c Y    a X    b		Z    c Y    a X    b		Z    c Y    b X    a		X    b Z $\wedge$ c = $13(1)^\circ$

Table 4. Chemical composition of parascholzite

	theoretical $\text{CaZn}_2(\text{PO}_4)_2 \cdot 2\text{H}_2\text{O}$	parascholzite
ZnO	41.02	40.1
MnO	—	1.4
FeO	—	0.5
CaO	14.13	12.8
$\text{P}_2\text{O}_5$	35.77	35.7
$\text{H}_2\text{O}$	9.08	8.8
	100.00	99.3

Accuracy of data: plus or minus 3% of the amount present.

formula  $\text{Ca}_3\text{Zn}(\text{OH})_2(\text{PO}_4)_2 \cdot \text{H}_2\text{O}$  with  $Z = 2$ . In 1956 Strunz and Tennyson published a new description of scholzite in which the mineral was described as being orthorhombic,  $Pbmm$  or  $Pbnm$ , with  $a = 17.14$ ,  $b = 22.19$ , and  $c = 6.61\text{\AA}$ . A new formula was given as  $\text{CaZn}_2(\text{PO}_4)_2 \cdot 2\text{H}_2\text{O}$  with  $Z = 4$ . It was also noted that the powder diffraction patterns of some crystals differed slightly.

Our investigation shows that at Hagendorf and other localities scholzite and parascholzite occur together, sometimes within the same crystal as syntaxial intergrowths. This fact explains some of the confusing and contradictory data previously reported for scholzite, the data having been obtained from crystals containing parascholzite lamellae or even from pure parascholzite. To resolve the discrepancies and to confirm that scholzite and parascholzite are indeed distinct species, it was necessary to re-investigate the

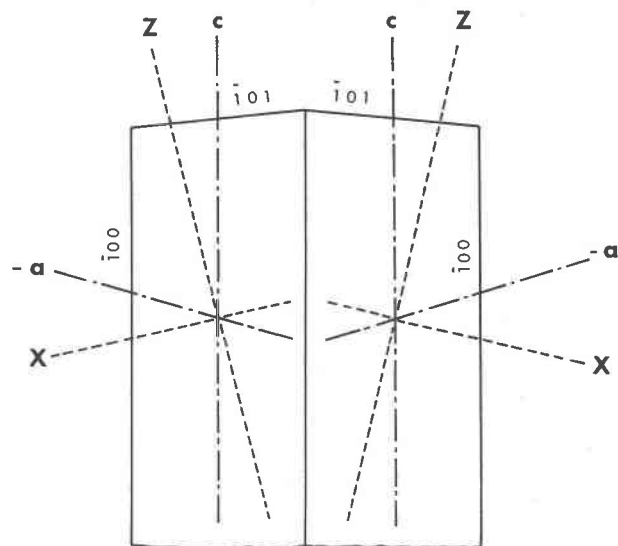


Fig. 4. Section parallel to (010) of a sample twin of parascholzite showing the orientation of the optical elements.

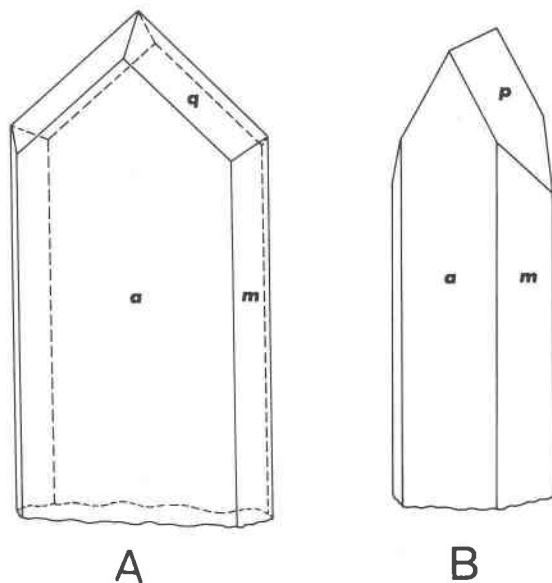


Fig. 5. Two crystal habits of scholzite from Reaphook Hill.

former mineral. Unfortunately, we could not find any scholzite crystals free of admixed parascholzite on the specimens from the type locality. All examined crystals of scholzite from Hagendorf had parascholzite lamellae that were clearly visible under the microscope and parascholzite lines were easily identified in the powder diffraction patterns.

The large, well-developed crystals of scholzite from Reaphook Hill, Australia, were then chosen for study. They had parallel extinction, their powder pattern lacked parascholzite lines, and the single-crystal study indicated an orthorhombic unit cell. However, careful examination under the microscope with the highest power objective showed that the crystals from Reaphook Hill also have parascholzite lamellae included. They are, however, thin and the amount of the admixed parascholzite is too small to manifest itself in the powder pattern or on the precession photographs.

#### Crystallography

The large well-developed crystals from Reaphook Hill (Fig. 5) are up to one cm long and about 1.0 mm in cross-section. They are elongated parallel to [001] and the forms observed with the optical goniometer are  $a$  {100},  $k$  {110},  $m$  {130},  $q$  {231}, and  $p$  {061}. The observed  $\phi$  and  $\rho$  angles are given in Table 5.

Two slightly different habits of elongated crystals of scholzite were observed. The crystals shown in Figure 5(a) are found on the specimen where only scholzite crystals were developed. The crystals in

Table 5. Angle table for scholzite from Reaphook Hill, Australia

Form	Orthorhombic, $a=17.178$ , $b=22.24$ , $c=6.681$			
	Measured		Calculated	
	$\phi$	$\rho$	$\phi$	$\rho$
a(100)	90°	90°	90°00'	90°00'
k(110)	52°26'	90°	52°19'	90°00'
m(130)	23°58'	90°	23°20'	90°00'
q(231)	41°02'	49°54'	40°47'	49°58'
p(061)	0°	60°50'	0°00'	60°58'

Figure 5(b) are from the specimen where both parascholzite and scholzite crystals occur together. We do not know the reason for the different habits. The crystals from both specimens have thin parascholzite lamellae as described in the previous section.

The unit cell and space group of scholzite from Reaphook Hill in Table 3 were determined by the precession method and are in agreement with those of Taxer (1975), who has confirmed them by crystal structure analysis. As reported by Taxer (1975), scholzite has a substructure with  $B = b/3$  and symmetry  $Pbcn$ . Hill *et al.* (1973) concluded from their single-crystal intensity data that the true symmetry of the supercell is  $P2_1/b$  ( $a$ -axis unique). Our crystals show no evidence for this and we suspect that the reported monoclinic intensity distribution results from the use of crystals contaminated with monoclinic parascholzite.

Unit cell dimensions of scholzite from Hagendorf (Table 3) were refined from Gandolfi powder data, and the space group was determined with the precession method on crystals composed of scholzite and parascholzite in syntaxial intergrowth.

Powder diffraction data for scholzite from Reaphook Hill are given in Table 2. As with parascholzite, the reflections were indexed with the aid of the single-crystal photographs. Comparing our pattern with that of Hill and Milnes (1974) for scholzite from the same locality, it is evident that the indexing is the same except for six reflections labelled (120), (210), (141), (152), (720), and (452) by Hill and Milnes. All of these are superstructure reflections ( $k \neq 3n$ ) and on our single-crystal photographs they are either absent or present but much too weak to appear in any powder pattern. Hill's line at 9.3Å indexed as "(120)" is probably the  $K\beta$  line of (200), which is the strongest  $K\alpha$  reflection in the scholzite pattern. Reflection "(141)" at 4.16Å is ( $\bar{3}11$ ) of parascholzite ( $d_{obs} = 4.158\text{Å}$ ), which is the third strongest reflection from

that mineral. Reflection "(452)" is properly indexed as (660). The remaining lines "(210), (152), and (720)" do not appear in our Guinier patterns, cannot be reasonably indexed using the single-crystal intensities, and must therefore be due to some minor impurity in Hill's sample. Other published powder data for scholzite show many of the same extraneous lines (Timchenko and Sidorenko, 1962; Staněk, 1966; Fransolet *et al.*, 1974; JCPDS pattern 13-445).

The powder data for synthetic scholzite deserve special attention, since they have been used to question the existence of glide symmetry in this material (Milnes and Hill, 1977). The pattern in question contains eight lines which are absent from our patterns of the natural mineral, namely "(120), (030), (031), (050), (141), (250), (122), and (222)". The second, third, and fourth reflections in this list have  $k$  odd and therefore violate the  $b$ -glide extinction rule in  $P2_1/b$ , which is the space group assumed for scholzite by Milnes and Hill. This led them to propose that some scholzites deviate from  $P2_1/b$  symmetry in having only approximate glide symmetry. However, reference to our Table 2 shows that "(031), (050), (141), (122), and (222)" are actually parascholzite lines and, in fact, the high intensity (60) of reflection "(141)" indicates that this sample was predominantly parascholzite. Reflection "(120)" is probably a  $K\beta$  line as described above. The case for variable symmetry in scholzite therefore rests upon a single weak powder reflection, "(030)", which, along with "(250)", can more reasonably be attributed to the presence of some minor contaminant.

#### Physical and optical properties

Scholzite is white to colorless with a white streak and vitreous luster. The specific gravity of scholzite from Reaphook Hill is 3.13(2) compared to the density of 3.10 g/cm<sup>3</sup> calculated from the ideal formula and our refined cell parameters. The Mohs hardness is 4. No cleavage was observed, but scholzite may show parting along the plane of syntaxy {100}. This is undoubtedly the origin of the good {100} cleavage reported by Strunz and Tennyson (1956). Scholzite does not fluoresce in ultraviolet light.

Table 3 summarizes the optical data for scholzite and compares our results for the Hagendorf material with those of Strunz (1950) and Strunz and Tennyson (1956). All Hagendorf scholzite contains parascholzite lamellae, but we were still able to determine refractive indices, the angle  $2V$ , and the orientation of the indicatrix using the Supper spindle stage. Also in Table 3 are included certain previously unreported

Table 6. Angle table for crystals composed of intergrowth of scholzite and parascholzite from Hagendorf, Germany

		SCHOLZITE orthorhombic a=17.178, b=22.24, c=6.681		PARASCHOLZITE monoclinic a=17.864, b=7.422, c=6.674, $\beta=106^{\circ}27'$			
measured $\phi$	$\varphi$	Form	calculated $\phi$	$\varphi$	Form	calculated $\phi$	$\varphi$
90°	90°	a (100)	90°00'	90°00'	a (100)	90°00'	90°00'
23°	90°	k (130)	23°20'	90°00'	k (110)	23°25'	90°00'
53°	90°	m (110)	52°19'	90°00'	m (310)	52°25'	90°00'
62°	90°	j (320)	62°45'	90°00'	j (410)	60°00'	90°00'
90°	9°	x (102)	90°00'	11°00'	x ( $\bar{1}02$ )	90°00'	5°44'
-90°	10°					y ( $\bar{1}01$ )	-90°00'
0°	43°	g (031)	0°00'	42°01'	g ( $\bar{1}11$ )	-5°59'	42°07'
20°	44°	o (131)	23°20'	44°27'	p (011)	18°10'	43°25'
-22°	44°					p ( $\bar{2}11$ )	-28°16'

Note: Unit cell dimensions used in calculation were determined on scholzite from Reaphook Hill (Table 5) and on parascholzite from Hagendorf (Table 1).

optical data for scholzite from Reaphook Hill. The parascholzite lamellae in Australian scholzite are so thin that they can be observed only with the strongest objective (UM 50x). Even at this magnification we could only see the lamellae as thin lines. The composition plane is {100} and lamellae show inclined extinction; they are too small to show the full inclined extinction of parascholzite, but are seen as darker or lighter lines during the rotation of the microscope stage, just before the host crystal becomes dark.

Our identification of these lamellae as parascholzite is based on the observation under the microscope; the inclined extinction, the composition plane being {100}, and the fact that refractive indices of lamellae and host crystal are practically identical.

The specific refractivity calculated from the ideal composition and constants of Mandarino (1976) and the Gladstone-Dale relationship is  $Kc = 0.188$ . It compares well with the  $Kp = 0.188$  calculated from the measured density and refractive indices of scholzite from Reaphook Hill.

#### Occurrence

Three distinct parageneses have been reported for scholzite. It is found as a primary product of crystallization in zinc and phosphate-bearing pegmatites. The only recorded example is at Otov, near Domažlice, Bohemia (Staněk, 1966). Scholzite is also found as a secondary mineral produced by alteration of primary phosphates in such pegmatites. The type locality at Hagendorf and the Transbaikalian occurrences (Timchenko and Sidorenko, 1962) belong in this category. In addition, it has been found as a secondary mineral produced by weathering and enrichment by circulating ground waters of sedimentary rocks con-

taining low grade zinc and phosphorus mineralization. Examples are Reaphook Hill (Hill *et al.*, 1973; Hill and Milnes, 1974) and Richelle, Belgium (Fransolet *et al.*, 1974).

Mention should also be made here of the industrial use of synthetic scholzite, a use which elevates the mineral above the status of a mere mineralogical curiosity. When the surface of steel is treated with calcium zinc phosphate solutions, a corrosion-resistant film of  $\text{CaZn}_2(\text{PO}_4)_2 \cdot 2\text{H}_2\text{O}$  is formed to a thickness of a few microns (Gebhardt and Neuhaus, 1964; Rausch *et al.*, 1973). Although this product is termed "scholzite" in the chemical engineering literature, it is obvious from the present work that some or all of it may be parascholzite.

#### Syntaxial intergrowths

Several crystals of scholzite from Hagendorf containing syntaxially intergrown parascholzite lamellae (Fig. 6) were studied with the microscope, optical goniometer, and precession camera. The lamellae have nearly the same refractive indices as the host scholzite but could be distinguished under crossed Nicols by their inclined extinction. The intergrowths have {100} as the composition plane and the *b*, *c*, and *a\**-axes of the two phases are parallel. A *b*-axis precession film of one such intergrowth is identical to the superimposed films of scholzite and parascholzite. The combined pattern is dimensionally orthorhombic with three orthogonal cell axes but shows Friedel symmetry  $2/m$ . It is likely that the monoclinic, pseudoorthorhombic scholzite of Strunz

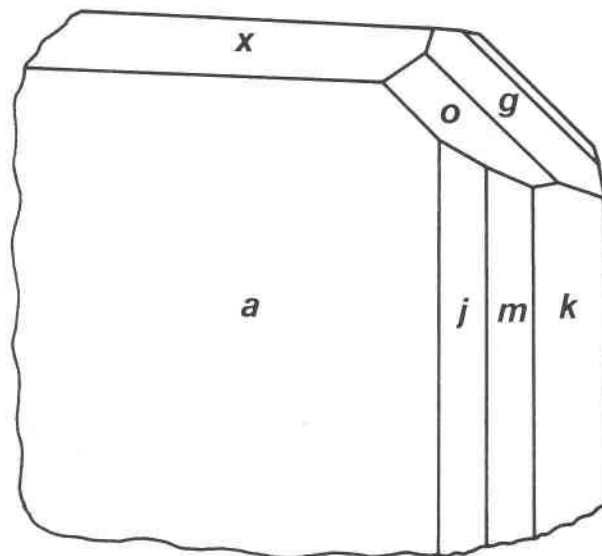


Fig. 6. Crystal from Hagendorf-Süd composed from scholzite and parascholzite in syntaxial intergrowth.

(1950) has its origin in the misinterpretation of diffraction photographs of these syntaxial intergrowths. Precession photographs of Hagendorf parascholzite usually also show weak reflections due to intergrown scholzite.

The accuracy of the goniometric measurements of the crystal faces was much lower than usual, the signals from faces in the [010] zone being especially poor. The reason for this seems to be that the faces are composed of many narrow faces or steps. Each of these narrow faces belongs to one lamella of parascholzite slightly protruding from the large face of the host scholzite crystal. We have failed in several attempts to prepare a thin section of an intergrowth crystal perpendicular to the *b*-axis. Such a section would have permitted a determination of which forms are developed on the lamellae and whether they are different from those on the host crystal. In Table 6 we give measured values of the angles  $\phi$  and  $\rho$  and compare them to values calculated for scholzite and parascholzite.

In scholzite and parascholzite the (100) plane is important in four respects. It is (1) the plane of the  $(\text{PO}_4 + \text{ZnO}_4)$  sheets (this has yet to be verified in the case of parascholzite), (2) the twin and composition plane of polysynthetically twinned parascholzite, (3) the plane normal to which stacking disorder occurs in both polymorphs, and (4) the interface or composition plane in scholzite–parascholzite intergrowths. The last three phenomena almost certainly arise from the first. The frequency with which the two polymorphs occur together, usually on the same specimen and often in the same crystal, suggests that their energies are similar. Likewise, the common occurrence of polysynthetic twins and syntaxial intergrowths suggests that the energies of these composite crystals are not far removed from those of single-crystals of the pure polymorphs.

#### Acknowledgments

We would like to thank Mr. R. A. Ramik for performing DTA/TGA and for interpretation of the results, and Dr. Paul Moore

and Dr. Karlheinz Taxer for the critical reading of the manuscript. Ms. Julie Norberg provided the water determination by Penfield method.

#### References

- Czaya, R. (1972) Dehydration and transformation phases of scholzite  $\text{CaZn}_2(\text{PO}_4)_2 \cdot 2\text{H}_2\text{O}$ . *Acta Crystallographica*, B28, 322–323.
- Fransolet, A. M., Jedwab, J., and van Tassel, R. (1974) La scholzite de Richelle, mineral nouveau pour la Belgique. *Annales de la Societe Geologique de Belgique*, 97, 321–330.
- Gebhardt, M. and Neuhaus, A. (1964) Neue Untersuchungen an Phosphatierungsschichten auf Metallen. *Die Naturwissenschaften*, 51, 358.
- Hill, R. J. and Milnes, A. R. (1974) Phosphate minerals from Reaphook Hill, Flinders Ranges, South Australia. *Mineralogical Magazine*, 39, 684–695.
- Hill, R. J., Johnson, J. E., and Jones, J. B. (1973) Scholzite and other phosphate minerals from Reaphook Hill, South Australia. *Neues Jahrbuch fur Mineralogie Monatshefte*, 1–8.
- Mandarino, J. A. (1976) The Gladstone–Dale relationship—Part I: Derivation of new constants. *Canadian Mineralogist*, 14, 498–502.
- Milnes, A. R. and Hill, R. J. (1977) Preparation of synthetic scholzite, hopeite and tarbuttite and their comparison with natural material. *Neues Jahrbuch fur Mineralogie Monatshefte*, 25–38.
- Rausch, W., Claude, P., and Huhn, G. (1973) Phosphatizing of steel in zinc-calcium phosphate systems. In N. Ibl, Ed., *Proceedings of the Congress of the International Union of Electrodeposition Surface Finishing*, 8th, 1972, 308–312. Forster-Verlag AG, Zurich.
- Stanek, J. (1966) Scholzit a hurlbutit z pegmatitu od Otava u Domazlic. *Casopis pro Mineralogii a Geologii*, 11, 21–26.
- Strunz, H. (1950) Scholzit, eine neue Mineralart. (abstr.) *Fortschritte der Mineralogie*, 27, 31.
- Strunz, H. and Tennyson, Ch. (1956) Kristallographie von Scholzit,  $\text{CaZn}_2(\text{PO}_4)_2 \cdot 2\text{H}_2\text{O}$ . *Zeitschrift fur Kristallographie*, 107, 318–330.
- Taxer, K. J. (1970) Die Kristallstruktur des Minerals Scholzit. *Die Naturwissenschaften*, 57, 192.
- Taxer, K. (1975) Structural investigations on scholzite. *American Mineralogist*, 60, 1019–1022.
- Timchenko, T. I. and Sidorenko, G. A. (1962) Nakhodki tsinkovikh fosfatov v pegmatitakh Zabaiykalya. *Trudi Mineralogicheskogo Muzeya, Akademiya Nauk SSSR*, 13, 219–223.

*Manuscript received, October 28, 1980;  
accepted for publication, February 10, 1981.*